

1 Investigation of particle antiparticle elliptic flow difference  
2 at STAR experiment\*

3 MARIA STEFANIAK (FOR THE STAR COLLABORATION)

4 1) Faculty of Physics, Warsaw University of Technology  
5 Koszykowa 75, 00-662 Warszawa, Poland,  
6 2) Subatech - IMT Atlantique  
7 4 rue Alfred Kastler, 44300 Nantes, France

8 The azimuthal anisotropy in particle emission in the transverse plane,  
9 known as anisotropic flow, is used to study the properties of strongly inter-  
10 acting hot and dense medium created in heavy-ion collisions. Anisotropic  
11 flow coefficients are the key observables which reflect the viscous hydro-  
12 dynamic response to the initial spatial anisotropy, produced in the early  
13 stages of the collision. In previous studies performed by the Solenoidal  
14 Tracker At RHIC (STAR) collaboration at the Relativistic Heavy Ion Col-  
15 lider (RHIC) the increase of the elliptic flow ( $v_2$ ) difference between par-  
16 ticles and antiparticles at the lower collision energies has been observed.  
17 In these proceedings we present the measurement of the two-particle el-  
18 liptic and triangular flow correlations for identified particles performed by  
19 the STAR experiment. Our measurements are compared with the EPOS  
20 model simulations as well.

21 **1. Introduction**

22 Studying the properties of the strongly interacting matter is one of the  
23 major milestones for current heavy ion research. Various experimental fa-  
24 cilities have been designed to investigate the Quantum Chromo-Dynamical  
25 (QCD) phase diagram such as Beam Energy Scan (BES) [1] at Relativis-  
26 tic Heavy Ion Collider (RHIC) [2]. This program is at the forefront of  
27 experimental efforts designed to map the thermodynamical and transport  
28 properties of strongly interacting QCD matter. Flow is an observable char-  
29 acterizing the shape of the expanding matter [4, 5]. It is very sensitive  
30 to the properties of the system at very early time of its evolution. In the  
31 previous studies performed by STAR collaboration [3, 8, 9] the increase of  
32 the difference in elliptic flow of particles and antiparticles with the decrease  
33 of the collision energy has been observed. However, the sources of these  
34 phenomena were not well understood.

---

\* Presented at XIV Workshop on Particle Correlation and Femtoscopy

## 2. Measurements

The two-particle correlations (2PCs) are obtained by averaging over all unique combinations in single event, and then over all events [6]. All particles from one collision are divided into two groups - subevents  $a$  and  $b$  considering their pseudorapidity ( $\eta$ ). The 2PCs are calculated with the following formula:

$$c_n\{2\} = \langle\langle 2 \rangle\rangle_{a|b} = \langle\langle e^{in(\phi_1^a - \phi_2^b)} \rangle\rangle = \frac{\langle Q_{n,a} Q_{n,b}^* \rangle}{\langle M_a M_b \rangle} \quad (1)$$

where:  $n$  - flow harmonic,  $\phi$  - particle's azimuthal angle,  $M_{a/b}$  - multiplicity of particles in subevents  $a$  and  $b$ , and  $Q_{n,a/b} \equiv \sum_i e^{in\phi_i^{a/b}}$  - flow vector. This leads to the following cumulant-based definition of harmonic flow  $v_n$ :

$$v_n\{2\} = \sqrt{c_n\{2\}} \quad (2)$$

The flow dependence on the transverse momentum of particles is given by:

$$v_n(p_T) = v_n^2(p_T, p_T^{ref}) / \sqrt{v_n^2(p_T^{ref}, p_T^{ref})}, \quad (3)$$

where  $p_T^{ref}$  is the transverse momentum of the reference particle.

The 2PCs carry flow and non-flow (NF) contribution: short-range (HBT, decays of resonances, etc.) and long-range (momentum-conservation, di-jets, etc.) [6, 7]. In order to suppress NF impact on the measurements, the  $\Delta\eta$  between subevents is introduced. In the Figure 1  $v_n\{2\}$  measurements with different gap in the pseudorapidity are presented. The bigger  $\Delta\eta$  is used the more NF contribution is suppressed. It is more pronounced for peripheral events.

Calculated flow measurements are scaled with the number of constituent quarks of given hadron (NCQ-scaling) in function of transverse kinetic energy ( $KE_T$ ) [12].

For identification of particles the Time Projection Chamber (TPC) and Time-Of-Flight (TOF) information were used in the momentum range  $p$  (GeV/c)  $\leq 4.0$  and rapidity  $|y| < 1.0$ .

## 3. Results and discussion

The  $p_T$ -differential two-particle correlations for various flow harmonics were measured for the data collected by STAR at two collision energies:  $\sqrt{s_{NN}} = 200$  GeV and 39 GeV. For all flow measurements only statistical errors are taken into account. The  $p_T$ -differential two-particle correlations  $v_2\{2\}$ ,  $v_3\{2\}$  and  $v_4\{2\}$  for identified hadron in centrality range 10% – 40%,

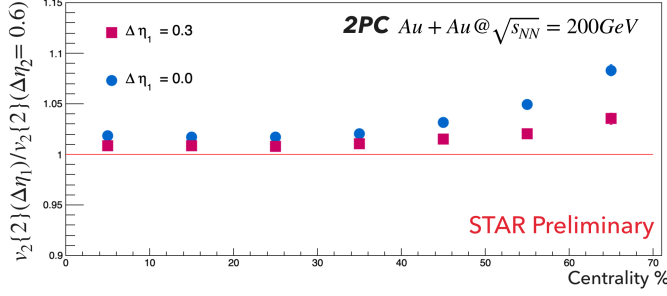


Fig. 1: Ratio of the centrality dependent  $v_2\{2\}$  with  $\Delta\eta_1 = 0.0$  and  $0.3$  to  $v_2\{2\}$  with  $\Delta\eta_2 = 0.6$  for Au+Au collisions at  $\sqrt{s_{NN}} = 200$  GeV. The transverse momentum range:  $0.2 < p_T$  (GeV/c)  $< 4.0$ .

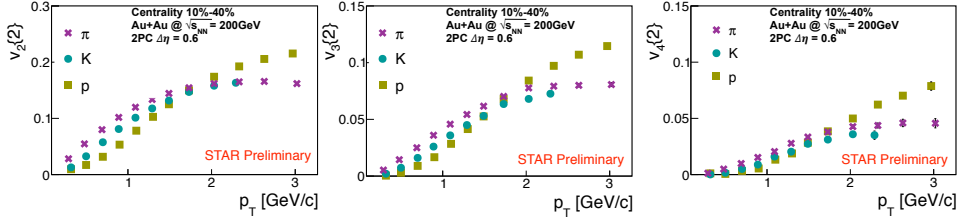


Fig. 2:  $v_2\{2\}$ ,  $v_3\{2\}$  and  $v_4\{2\}$  in function of  $p_T$  for  $\Delta\eta = 0.6$ , centrality 10% – 40% for Au+Au collisions at  $\sqrt{s_{NN}} = 200$  GeV.

65 measured for Au+Au collisions at  $\sqrt{s_{NN}} = 200$  GeV are shown in Fig. 2.  
 66 The mass dependence is visible for all studied harmonics. The NCQ( $KE_T$ )-  
 67 scalings are presented in Fig.3. All studied harmonics  $v_n\{2\}/n_q^{n/2}$  scales  
 68 with  $KE_T/n_q$ .

69 The elliptic and triangular flow for identified hadrons measured in Au+Au  
 70 collisions at  $\sqrt{s_{NN}} = 39$  GeV are presented in Fig.4 and 5. Both  $v_n$  show  
 71 similar trends.

72 The ratios of particles to antiparticles elliptic and triangular flow are  
 73 shown in Fig.6 and 7. The differences between protons' and antiprotons'

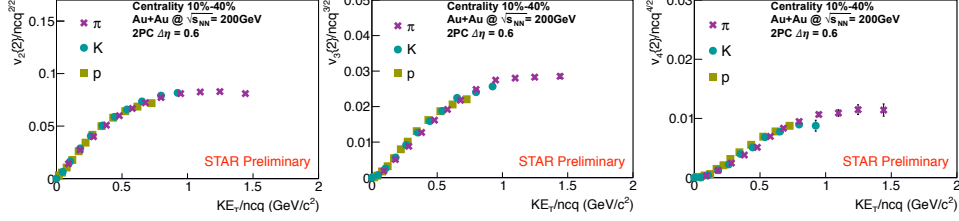


Fig. 3: Scaling with number of constituent quarks ( $ncq^{n/2}$ , where  $n$  is the flow harmonic) of  $v_2\{2\}$ ,  $v_3\{2\}$  and  $v_4\{2\}$  in function of  $KE_T/ncq$  with  $\Delta\eta = 0.6$ , centrality 10% – 40% for Au+Au collisions at  $\sqrt{s_{NN}} = 200$  GeV.

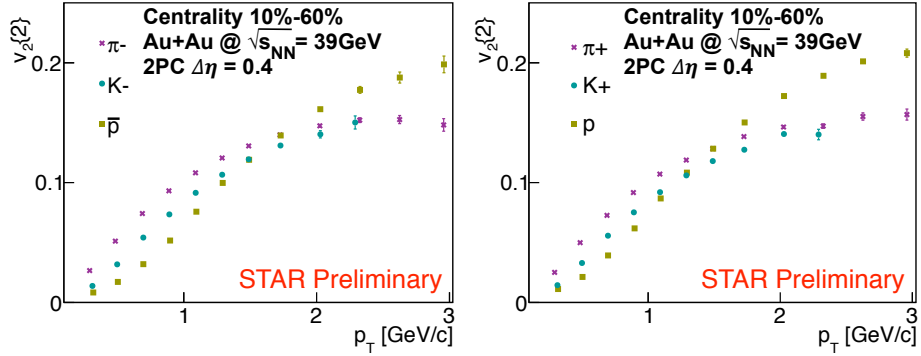


Fig. 4: Particles (left panel) and antiparticles (right panel)  $v_2\{2\}$  in function of  $p_T$  for  $\Delta\eta$  gap equals 0.4, centrality 10% – 60% for Au+Au collisions at  $\sqrt{s_{NN}} = 39$  GeV.

74 elliptic flow, especially for lower  $p_T$ , are significant. On the other hand, the  
 75 available statistic for introduced cuts and  $\Delta\eta$  does not allow for such clear  
 76 conclusion in case of triangular flow.

77 The performed experimental studies of elliptic flow are compared with  
 78 results obtained using simulated EPOS model data [10, 11]. Hydrodynam-  
 79 ical evolution included in the model is based on the Equation of State cor-  
 80 responding to the baryonic chemical potential ( $\mu_B$ ) equals to zero. The  
 81 research was done for two collision energies  $\sqrt{s_{NN}} = 39$  GeV and 200 GeV,

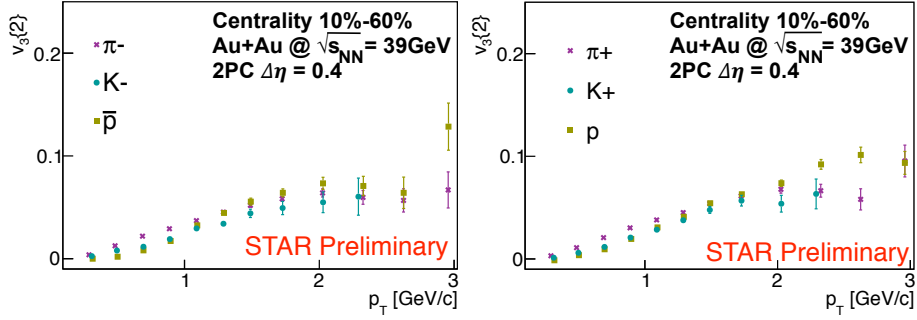


Fig. 5: Particles (left panel) and antiparticles (right panel)  $v_3\{2\}$  in function of  $p_T$  for  $\Delta\eta = 0.4$ , centrality 10%–60% for Au+Au collisions at  $\sqrt{s_{NN}} = 39$  GeV.

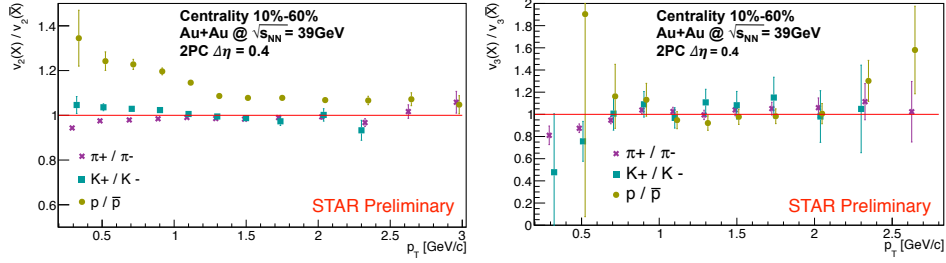


Fig. 6: Ratio of  $v_2\{2\}$  (left panel) and  $v_3\{2\}$  (right panel) of particles to antiparticles,  $\Delta\eta$  gap equals 0.4, centrality 10%–60% for Au+Au collisions at  $\sqrt{s_{NN}} = 39$  GeV.

82 is presented in Fig. 7.

83 The EPOS model does not reproduce pions' elliptic flow for  $p_T > 2$   
 84 GeV/c at  $\sqrt{s_{NN}} = 200$  GeV, while at  $\sqrt{s_{NN}} = 39$  GeV the model fails in  
 85 describing  $v_2$  of  $\pi$ 's in the whole  $p_T$  range. Comparisons with the experi-  
 86 mental flow measurements can be a useful constrain for the future model  
 87 development.

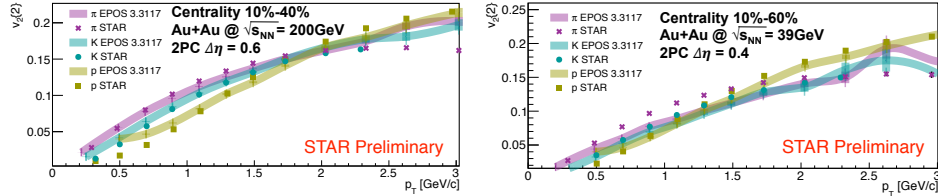


Fig. 7:  $v_2\{2\}$  of identified particles at  $\sqrt{s_{NN}} = 200$  GeV (left panel) and  $\sqrt{s_{NN}} = 39$  GeV (right panel). STAR experimental data are compared with EPOS 3.3117 simulated data.

88

#### 4. Conclusion

89 In summary, we have presented a comprehensive set of STAR  $v_n$  mea-  
 90 surements for Au+Au collision energies  $\sqrt{s_{NN}} = 39$  GeV and 200 GeV.  
 91 The mass dependence of all studied harmonics is visible. The NCQ( $KE_T$ )-  
 92 scaling works for gold ion collisions at  $\sqrt{s_{NN}} = 200$  GeV, while it seems  
 93 to be broken at  $\sqrt{s_{NN}} = 39$  GeV by protons. This could indicate the  
 94 various origins of these baryons. Elliptic flow of protons is larger than for  
 95 antiprotons at  $\sqrt{s_{NN}} = 39$  GeV. In the case of triangular flow, which is a  
 96 fluctuation-driven quantity, the differences are not that relevant.

#### REFERENCES

- 97 [1] Grazyna Odyniec: Journal of Physics Conference Series 455(1):2037  
 98 [2] V.A. Okorokov: Eur. Phys. J. Web of Conf. 158, 01004 (2017)  
 99 [3] STAR Collaboration: Phys. Rev. C 93, 014907 (2016)  
 100 [4] R. Snellings: New J.Phys.13:055008,2011  
 101 [5] Y. Pandit: 2013 J. Phys.: Conf. Ser. 420 012038  
 102 [6] J. Jia, Mingliang Zhou, Adam Trzupek: Phys. Rev. C 96, 034906 (2017)  
 103 [7] A. Bilandzic, Raimond Snellings, Sergei Voloshin: Phys.Rev.C83:044913,2011  
 104 [8] STAR Collaboration: Phys. Rev. Lett 112, 162301 (2014)  
 105 [9] STAR Collaboration: Phys.Rev.Lett. 110, 142301 (2013)  
 106 [10] Werner, K. et al.: Adv.Ser.Direct.High Energy Phys. 29 (2018)  
 107 [11] Werner, K. et al. : J. Phys.: Conf. Ser. 1070 012007 2018  
 108 [12] J. Dunlop, M.A. Lisa, P. Sorensen: Phys.Rev. C84 (2011) 044914